

RSC Advances



This is an *Accepted Manuscript*, which has been through the Royal Society of Chemistry peer review process and has been accepted for publication.

Accepted Manuscripts are published online shortly after acceptance, before technical editing, formatting and proof reading. Using this free service, authors can make their results available to the community, in citable form, before we publish the edited article. This *Accepted Manuscript* will be replaced by the edited, formatted and paginated article as soon as this is available.

You can find more information about *Accepted Manuscripts* in the [Information for Authors](#).

Please note that technical editing may introduce minor changes to the text and/or graphics, which may alter content. The journal's standard [Terms & Conditions](#) and the [Ethical guidelines](#) still apply. In no event shall the Royal Society of Chemistry be held responsible for any errors or omissions in this *Accepted Manuscript* or any consequences arising from the use of any information it contains.

COMMUNICATION

Wettability of Graphene Nanoribbons/ Single-Walled Carbon Nanotubes Hybrid Film

Cite this: DOI: 10.1039/x0xx00000x

Xiaokun Fan,^{†, a} Li Tao,^{†, b} Ya Deng,^b Gang Wang,^b Jian Zhang,^b Yun Zhao,^c Wenbin Huang,^d Huiyou Zhao,^a Lianfeng Sun^{b, *}Received 00thXXXX XXXX,
Accepted 00thXXXX XXXX

DOI: 10.1039/x0xx00000x

www.rsc.org/

In this work, the surface part of single-walled carbon nanotubes (SWNTs) film were unzipped by sputtering Zn/HCl process, and the wettability of this graphene nanoribbons (GNRs)/SWNTs hybrid film was investigated. The contact angle of water droplets on the hybrid films is ~ 113.0°, which is different from that on pristine SWNTs film (~ 121.8°). The mechanism of this variation is discussed. Combining the unique properties of GNRs and SWNTs film, this kind of hybrid film is of great application potential.

Introduction

Graphene is the thinnest two-dimensional atomic crystal with outstanding mechanical and electronic properties,¹⁻⁴ and has attracted considerable attention since its successful isolation from graphite.² The perfect structure of the carbon atoms which arrange in the hexagonal lattice makes the electrons in graphene behave like the massless Dirac fermions, leading to the carrier mobility much higher than those of silicon and sub-micrometer ballistic transport in room temperature.⁵ However, the zero-bandgap feature of graphene limits its application in electronics. One promising approach to open the band gap is to produce GNRs due to the quantum confinement of electrons. Theoretical investigation suggests that the band gap is inversely proportional to the width of GNRs.⁶ The on/off ratio of sub-10 nm wide GNR-based field-effect transistors could be as high as 10⁶, thus providing application potential in all-carbon electronics.⁷ There are several methods to synthesize GNRs, among which unzipping carbon nanotube is an ideal one resulting in width and morphology controllable GNRs.⁸⁻¹³

Previous studies have shown that particle bombarding and irradiation on carbon nanomaterials could modify their

microstructures.¹⁴⁻¹⁷ In 2011, Dimiev et al. found that sputter-coating graphene and graphene oxide with zinc and dissolving the Zn with dilute acid can remove one graphene layer and leaves the lower layers intact.¹⁸ Considering the similar *sp*² carbon configuration of grapheme and single-walled carbon nanotube (SWNT), the similar methods may be used to unzip SWNT into GNR. Recently, Wei et al. used this method to produce an intramolecular junction by the controllable unzipping of SWNTs, which combine a GNR and a SWNT in a one-dimensional nanostructure.¹⁹ Gong et al. used similar method to fabricate array structures of narrow GNRs and measured their electrical transport properties.²⁰ Theorists have predicted that the unzipped and partially unzipped SWNTs could have intriguing electronic properties.^{21, 22} For instance, Santos et al. showed that the GNRs will behave as transparent contacts for the SWNTs in seamless SWNT/GNR heterojunctions and huge magnetoresistance will exist in the junctions.²¹

The wettability, which has been researched in many fields recently, is one of the most important characteristics of a solid interface. It can reflect the changes of characteristics of a solid surface, including the chemical composition and the geometric structure. The wettability has a broad influence on the applications of materials for various industries, such as biomedical, automobile and paint industries.²³⁻³⁰

In this Communication, we will report the fabrication of GNRs/SWNTs hybrid films (GSHFs) through zinc sputtering on the SWNT films, and study the wettability of this hybrid films.

Experimental

The individual disperse SWNTs and SWNT films were fabricated by floating catalytic chemical vapor deposition (FCCVD).³¹⁻³³ As catalyst source, ferrocene/ sulfur powder is heated to 65-75°C and flowed into a reaction zone by the mixture of 1000 sccm argon and 1-10 sccm methane. The temperature of the catalyst and the flow of the methane can be tunable with different samples.³⁴ The quality of the SWNTs can be studied by Raman spectroscopy and scanning electron microscopy (SEM). The micro-Raman measurements were performed with Renishaw inVia Raman Spectroscope under ambient conditions with the laser excitation of 514.5 nm (2.41 eV) induced by argon ion laser. The laser power is controlled at ~1 mW and the spatial resolution of laser spot is ~1 μm. The SEM measurements were taken under high vacuum (~10⁻³ Pa or lower) and the accelerating voltage is set at 3 kV using the Hitachi S-4800 field-emission system. For the disperse SWNT samples, we will immerse the samples into the de-ionized water to make the SWNTs adhere to the silicon wafers tightly, followed by air drying. After that, the SWNTs were sputtered by Zn (KJLC Lab-18, Lesker). After the pressure of the sputtering chamber reached 10 mTorr, pre-sputtering of Zn target was performed for 10 min to remove the impurities on the Zn target at a radio frequency (RF) power of 100 W, and then the Zn sputtering was performed at a RF power of 100 W for 10 min. After that, the SWNT samples were put into the dilute HCl (0.1 M) to dissolve the Zn residue. When the reaction is complete, the samples were taken out and rinsed with de-ionized water for several times. Finally, the samples were dried again in the air. For the SWNT films, the original SWNT films (O-SWNTFs) are fabricated by depositing SWNTs upon the silicon wafers directly with a duration of 2.5h. Since the structure of O-SWNTFs is very fluffy, we will condense the SWNT bundles by dropping the ethanol on to the films,³⁵ and then the films will be dried in the air. After that, the condensed SWNT films (C-SWNTFs) are processed in the same way as the disperse SWNT samples and dried in the air.

Results and discussion

By adjusting the parameters of the FCCVD system such as the catalyst sublimation temperature and the deposition duration to the optimized ones, we have obtained the disperse SWNT of high quality. Figure 1 shows typical atomic force microscope (AFM) images of pristine and unzipped SWNT, and the corresponding height profiles. It is obvious that the SWNTs are mostly individual ones rather than in the form of bundles. The heights of the pristine SWNT are 1.74/1.96 nm, respectively, which is consistent with our group's earlier report.³² The heights of the unzipped SWNT are 0.99/1.05 nm, respectively, indicating that the SWNTs are successfully unzipped into GNRs.

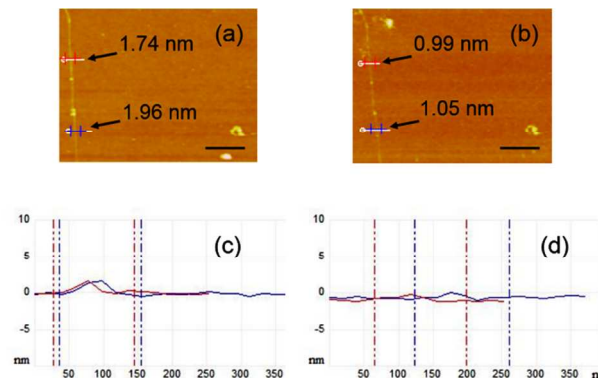


Figure 1. Typical AFM images of pristine (a) and unzipped (b) SWNT. The corresponding height profiles (c), (d) along the marked lines displayed in (a), (b). The heights are 1.74, 1.96 nm for pristine SWNT and 0.99, 1.05 nm for unzipped SWNT, respectively. The scale bar is 500 nm.

Figure 2 (a) shows a typical SEM image of the O-SWNTF on the silicon wafers. We can see that the O-SWNTFs are very fluffy. After ethanol dropping, the films get condensed, as shown in figure 2 (b). We have measured the contact angles (CAs) of de-ionized water droplets (1 μL) on O-SWNTFs and C-SWNTFs (OCA20 CA, Dataphysics), as shown in insets of figure 2 (a) and (b), respectively. The CA decreases from 136.4° to 124.1° after ethanol dropping. The accuracy of the CA measurements is higher than 1°. In order to confirm the characteristics of SWNTs wouldn't be changed by dropping the ethanol, we take the Raman spectra of these two kinds of films. Raman spectroscopy, known as a convenient and non-destructive technique, is widely used in probing the microstructures of carbon materials.³⁶ Figure 2 (c) shows typical Raman spectra of the O-SWNTF and C-SWNTF. We can see that the D peak of the SWNT films can almost be ignored, which proves that the SWNT films are of high quality. Furthermore, these two Raman spectra show remarkable similarity, indicating that the ethanol wouldn't influence the characteristics of SWNT films.

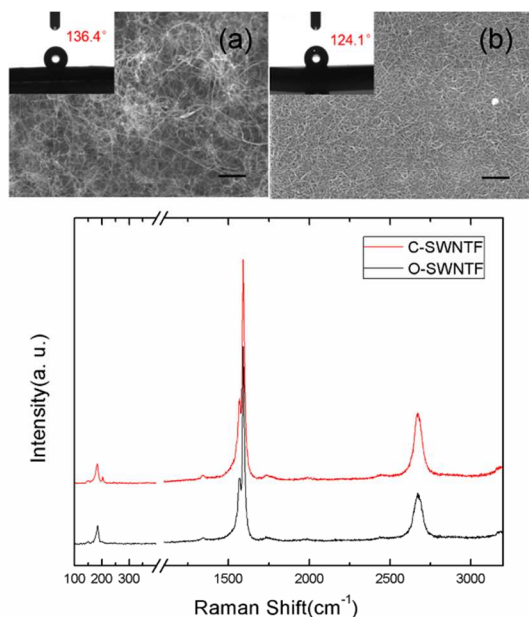


Figure 2. (a) A typical SEM image of the original SWNT film (O-SWNTF) which was fabricated by depositing SWNTs upon the silicon wafer directly, the inset is the contact angle (CA) of de-ionized water droplet on the O-SWNTF. (b) A typical SEM image of the condensed SWNT film (C-SWNTF) which was condensed by dropping ethanol on the O-SWNT, the inset is the CA of water droplet on the C-SWNTF. The scale bar is 1 μm . (c) Typical Raman spectra of the O-SWNTF (black) and the C-SWNTF (red), the remarkable similarity of these two Raman spectra indicates that the ethanol does not influence the characteristic of SWNT films.

The wettability of a solid surface, however, is strongly influenced both by its chemical composition and by its geometric structure (or surface roughness).³⁷⁻⁴⁰ If the films are sufficiently rough that the liquid may trap air, which could induce a composite surface effect. In this case, the relationship between the CA of the flat surface θ and that of the suitably rough surface θ_r is expressed by Cassie and Baxter equation:⁴¹

$$\cos \theta_r = r \cdot f_1 \cos \theta - f_2, \quad (1)$$

where r is the roughness factor (which is defined as the ratio of the actual surface area of a rough surface to the projected area), f_1 and f_2 are the fractions of the nanotubes and air on the O-SWNTFs, respectively. The Cassie and Baxter equation indicates that the CA θ_r increases with an increasing fraction of air (f_2).⁴² However, the as-grown SWNT films are also condensed when they were immersed into water. In order to eliminate the influence of water when the SWNT films are rinsed and confirm the decrease of the CAs of water droplet on GSHFs are not introduced by the water, we drop the ethanol on to the O-SWNTFs, as the figure 2 (b) shows, the SWNT bundles are much tighter just like the films which are picked out from water, and the CAs of water droplet on these two kinds of condensed SWNT films are same.

When the C-SWNTFs were dry, we tested the static CA of the water droplet on the C-SWNTFs before sputtering, firstly. As a control experiment, we also tested the CAs of water droplet on C-SWNTFs which were immersed into the dilute HCl without sputtering Zn. Comparing these two kinds results of CA measurements, we find no obviously differences, which indicates the HCl has little effects on the wettability of C-SWNTFs. When the GSHFs were dry, we tested the CAs of the water droplet on the GSHFs again. As shown in figure 3, the CAs decrease obviously after the SWNT films were processed.

Compared with the C-SWNTFs, the CAs of water droplets on the graphene films are smaller. Large-area monolayer graphene films have been synthesized by chemical vapour deposition (CVD) on Cu foils using the methane as the precursor at the 1030 $^{\circ}\text{C}$. Figure 3(d) shows the Raman spectra of graphene sample. We can see that the Raman spectra show typical features of monolayer graphene: (i) a ~ 2.64 2D-to-G intensity ratio and (ii) a symmetric 2D band with a full width at half maximum of $\sim 39.17 \text{cm}^{-1}$.^{43,44} For the ignorable D-peak, the quality of the graphene film should be high. We test the CAs of the water droplets on graphene films, the result ($\sim 85.4^{\circ}$) is similar with other reports.^{45,46}

On the basis of Young's equation,⁴⁷ as we all know, the CA can be given as follows:

$$\gamma_s = \gamma_{sl} + \gamma_l \cdot \cos \theta, \quad (2)$$

where γ_s , γ_l and γ_{sl} represent the solid surface free energy, liquid surface free energy, and solid-liquid interfacial energy, respectively. θ is the CA between the solid surface and liquid. On the other hand, the work of adhesion between a solid surface and liquid W_{sl} can be described by eqn (3):

$$W_{sl} = \gamma_s + \gamma_l - \gamma_{sl}. \quad (3)$$

Combining eqns (2) and (3) results in eqn (4):⁴⁸

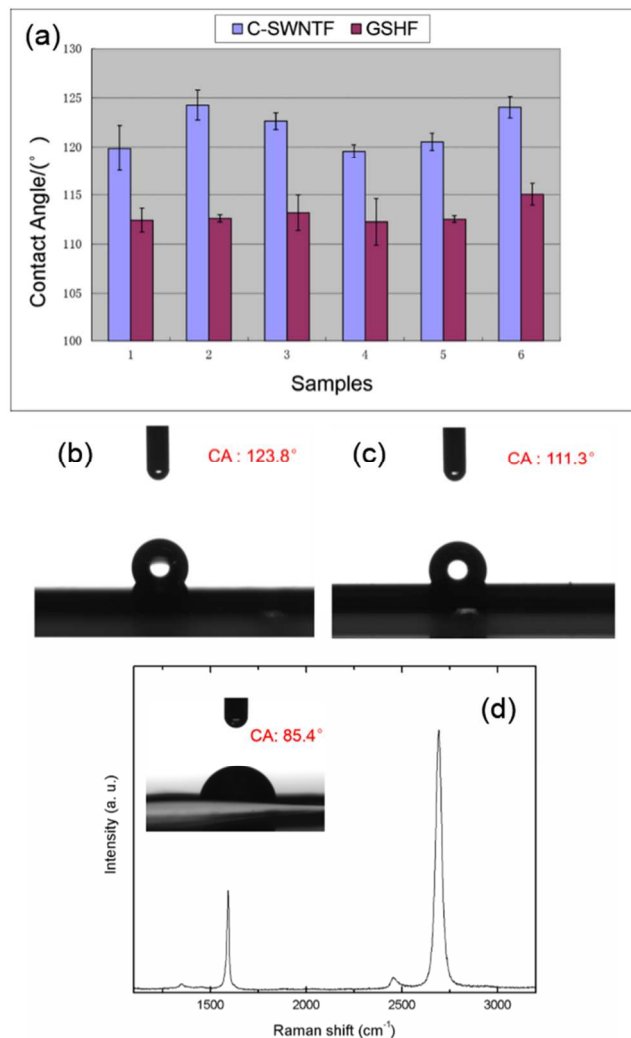


Figure 3. (a) The evolution of CAs of water droplets on C-SWNTFs and graphene nanoribbons/ single-walled carbon nanotubes hybrid films (GSHFs); (b) and (c) are the cross-sectional views of water droplet on the C-SWNTFs and GSHFs, respectively. (d) A typical Raman spectrum of graphene film, the inset is the cross-sectional views of water droplet on the graphene film.

$$W_{sl} = \gamma_l \cdot (1 + \cos \theta). \quad (4)$$

According to eq (4), the W_{sl} (graphene), W_{sl} (C-SWNTF) and W_{sl} (GSHF) are $1.08 \gamma_l$, $0.47 \gamma_l$ and $0.61 \gamma_l$, respectively. It is obvious that W_{sl} (graphene) is much higher than W_{sl} (C-SWNTF). So when the surface part of C-SWNTFs is unzipped by sputtering Zn/HCl process, the work of adhesion between the GSHF and water will increase and the CAs of water droplets on the GSHFs will decrease correspondingly. Another issue worth noting is that most SWNTs exist as the form of bundles in the SWNT films and the arrangement of SWNT bundles is completely random. Hence, the roughness of the GSHFs is much higher than that of graphene films. According to eqns (1) and (4), the CAs of water droplets on the GSHFs should be

bigger than that on the graphene film and smaller than that on the C-SWNTFs, which is consistent with our CA measurements.

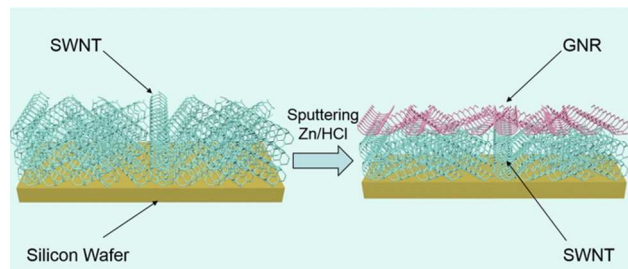


Figure 4. Schematic diagram of C-SWNTF unzipping into GSHF. The GSHF consists of GNR film in the surface part and C-SWNTF in the rest parts.

Conclusions

In summary, we have fabricated the GSHFs by the sputtering Zn/HCl method, and investigated the wettability of the GSHFs. As far as we know, it is the first time to fabricate this kind of GSHFs by the above method. We found that after unzipping, the wettability of SWNT films have changed, which can be demonstrated by the CA decreasing. Comparing unzipping the SWNT by the strong oxidant,^{9, 49} this method can keep the unique properties of the SWNT films without damaging the structure of the bottom part of SWNTs, and combine the properties of GNRs. We believe that this kind of GSHFs has greater application potential.

Acknowledgements

The authors sincerely thank National Center for Nanoscience and Technology for providing the fine work environment, experimental facility and technical support. This work was supported by National Science Foundation of China (Grant Nos. 10774032, 90921001), Key Knowledge Innovation Project of the Chinese Academy of Sciences on Water Science Research, Instrument Developing Project of the Chinese Academy of Sciences (Grant No. Y2010031).

Notes and references

^a School of Mechanical Electronic & Information Engineering, China University of Mining & Technology, Beijing 100083, China.

^b National Center for Nanoscience and Technology, Beijing 100190, China. E-mail: slf@nanoctr.cn; Fax: +8610-62656765; Tel: +8610-82545617.

^c Semiconductor Lighting Technology Research and Development Center, Institute of Semiconductors, Chinese Academy of Sciences, Beijing 100083, China.

^d Institute of Nanotechnology and Microsystems, Mechanical Engineering College, Shijiazhuang 050003, China

† These authors contributed equally to this work.

1. C. Lee, X. Wei, J. W. Kysar and J. Hone, *Science*, 2008, **321**, 385-388.
2. K. S. Novoselov, A. K. Geim, S. V. Morozov, D. Jiang, Y. Zhang, S. V. Dubonos, I. V. Grigorieva and A. A. Firsov, *Science*, 2004, **306**, 666-669.
3. X. Li, W. Cai, J. An, S. Kim, J. Nah, D. Yang, R. Piner, A. Velamakanni, I. Jung, E. Tutuc, S. K. Banerjee, L. Colombo and R. S. Ruoff, *Science*, 2009, **324**, 1312-1314.
4. S. Bae, H. Kim, Y. Lee, X. Xu, J. S. Park, Y. Zheng, J. Balakrishnan, T. Lei, H. R. Kim, Y. I. Song, Y. J. Kim, K. S. Kim, B. Ozyilmaz, J. H. Ahn, B. H. Hong and S. Iijima, *Nat.Nanotechnol.*, 2010, **5**, 574-578.
5. X. Du, I. Skachko, A. Barker and E. Y. Andrei, *Nat.Nanotechnol.*, 2008, **3**, 491-495.
6. L. Yang, C.-H. Park, Y.-W. Son, M. Cohen and S. Louie, *Phys. Rev. Lett.*, 2007, **99**, 186801.
7. X. Wang, Y. Ouyang, X. Li, H. Wang, J. Guo and H. Dai, *Phys. Rev. Lett.*, 2008, **100**, 206803.
8. L. Jiao, L. Zhang, X. Wang, G. Diankov and H. Dai, *Nature*, 2009, **458**, 877-880.
9. D. V. Kosynkin, A. L. Higginbotham, A. Sinitskii, J. R. Lomeda, A. Dimiev, B. K. Price and J. M. Tour, *Nature*, 2009, **458**, 872-876.
10. Z. X. Zhang, Z. Z. Sun, J. Yao, D. V. Kosynkin and J. M. Tour, *J. Am. Chem. Soc.*, 2009, **131**, 13460-13463.
11. L. Jiao, L. Zhang, L. Ding, J. Liu and H. Dai, *Nano Res.*, 2010, **3**, 387-394.
12. A. L. Elías, A. R. Botello-Méndez, D. Meneses-Rodríguez, V. Jehová González, D. Ramírez-González, L. Ci, E. Muñoz-Sandoval, P. M. Ajayan, H. Terrones and M. Terrones, *Nano Lett.*, 2009, **10**, 366-372.
13. F. Yu, H. Zhou, Z. Zhang, G. Wang, H. Yang, M. Chen, L. Tao, D. Tang, J. He and L. Sun, *Small*, 2013, **9**, 2405-2409.
14. F. Banhart, *Rep. Prog. Phys.*, 1999, **62**, 1181-1221.
15. L. Tao, C. Y. Qiu, F. Yu, H. C. Yang, M. J. Chen, G. Wang and L. F. Sun, *J. Phys. Chem. C*, 2013, **117**, 10079-10085.
16. Z. Xu, L. Chen, B. Zhou, Y. Li, B. Li, J. Niu, M. Shan, Q. Guo, Z. Wang and X. Qian, *RSC Adv.*, 2013, **3**, 10579.
17. O. V. Kharissova, B. I. Kharisov and E. G. de Casas Ortiz, *RSC Adv.*, 2013, **3**, 24812.
18. A. Dimiev, D. V. Kosynkin, A. Sinitskii, A. Slesarev, Z. Sun and J. M. Tour, *Science*, 2011, **331**, 1168-1172.
19. D. Wei, L. Xie, K. K. Lee, Z. Hu, S. Tan, W. Chen, C. H. Sow, K. Chen, Y. Liu and A. T. Wee, *Nat. Commun.*, 2013, **4**, 1374.
20. Y. Gong, M. Long, G. Liu, S. Gao, C. Zhu, X. Wei, X. Geng, M. Sun, C. Yang, L. Lu and L. Liu, *Phys. Rev. B*, 2013, **87**, 165404.
21. H. Santos, L. Chico and L. Brey, *Phys. Rev. Lett.*, 2009, **103**, 086801.
22. B. Huang, Y. W. Son, G. Kim, W. H. Duan and J. Ihm, *J. Am. Chem. Soc.*, 2009, **131**, 17919-17925.
23. J. Wang, Q. Cheng and Z. Tang, *Chem. Soc.Rev.*, 2012, **41**, 1111-1129.
24. M. Wu, H. Shuai, Q. Cheng and L. Jiang, *Angew. Chem. Int. Edit.*, 2014, **53**, 3358-3361.
25. J. Wang, L. Lin, Q. Cheng and L. Jiang, *Angew. Chem. Int. Edit.*, 2012, **51**, 4676-4680.
26. Q. Cheng, M. Wu, M. Li, L. Jiang and Z. Tang, *Angew. Chem. Int. Edit.*, 2013, **52**, 3750-3755.
27. Q. Cheng, M. Li, L. Jiang and Z. Tang, *Adv. Mater.*, 2012, **24**, 1838-1843.
28. J. Wang, Q. Cheng, L. Lin and L. Jiang, *ACS Nano*, 2014, **8**, 2739-2745.
29. W. Cui, M. Li, J. Liu, B. Wang, C. Zhang, L. Jiang and Q. Cheng, *ACS Nano*, 2014, **8**, 9511-9517.
30. Q. Cheng, L. Jiang and Z. Tang, *Accounts Chem.Res.*, 2014, **47**, 1256-1266.
31. W. Ma, L. Song, R. Yang, T. Zhang, Y. Zhao, L. Sun, Y. Ren, D. Liu, L. Liu, J. Shen, Z. Zhang, Y. Xiang, W. Zhou and S. Xie, *Nano Lett.*, 2007, **7**, 2307-2311.
32. F. Yu, H. Zhou, H. Yang, M. Chen, G. Wang and L. Sun, *Chem. Commun.*, 2012, **48**, 1042-1044.
33. L. Tao, G. Wang, F. Yu and L. Sun, *Chin. Sci. Bull.*, 2014, **59**, 2318-2323.
34. S. W. Pattinson, K. Prehn, I. A. Kinloch, D. Eder, K. K. K. Koziol, K. Schulte and A. H. Windle, *RSC Adv.*, 2012, **2**, 2909.
35. Z. Li, Y. Jia, J. Wei, K. Wang, Q. Shu, X. Gui, H. Zhu, A. Cao and D. Wu, *J. Mater. Chem.*, 2010, **20**, 7236.
36. M. S. Dresselhaus, A. Jorio, M. Hofmann, G. Dresselhaus and R. Saito, *Nano Lett.*, 2010, **10**, 751-758.
37. C. Neinhuis and W. Barthlott, *Ann. Bot.*, 1997, **79**, 667-677.
38. R. R. Netz and D. Andelman, *Phys. Rev. E*, 1997, **55**, 687-700.
39. M. Miwa, A. Nakajima, A. Fujishima, K. Hashimoto and T. Watanabe, *Langmuir*, 2000, **16**, 5754-5760.
40. A. Nakajima, K. Hashimoto, T. Watanabe, K. Takai, G. Yamauchi and A. Fujishima, *Langmuir*, 2000, **16**, 7044-7047.
41. A. B. D. Cassie and S. Baxter, *Trans. Faraday Soc.*, 1944, **40**, 0546-0550.
42. H. J. Li, X. B. Wang, Y. L. Song, Y. Q. Liu, Q. S. Li, L. Jiang and D. B. Zhu, *Angew. Chem. Int. Edit.*, 2001, **40**, 1743-1746.
43. Y. Gong, X. Zhang, G. Liu, L. Wu, X. Geng, M. Long, X. Cao, Y. Guo, W. Li, J. Xu, M. Sun, L. Lu and L. Liu, *Adv. Funct. Mater.*, 2012, **22**, 3153-3159.
44. A. C. Ferrari, J. C. Meyer, V. Scardaci, C. Casiraghi, M. Lazzeri, F. Mauri, S. Piscanec, D. Jiang, K. S. Novoselov, S. Roth and A. K. Geim, *Phys. Rev. Lett.*, 2006, **97**, 187401.
45. Y. J. Shin, Y. Wang, H. Huang, G. Kalon, A. T. Wee, Z. Shen, C. S. Bhatia and H. Yang, *Langmuir*, 2010, **26**, 3798-3802.
46. X. Dong, J. Chen, Y. Ma, J. Wang, M. B. Chan-Park, X. Liu, L. Wang, W. Huang and P. Chen, *Chem. Commun.*, 2012, **48**, 10660-10662.
47. Y. T., *Philosophical Trans. R. Soc. London*, 1805, **95**, 65-87.
48. S. Wang, Y. Zhang, N. Abidi and L. Cabrales, *Langmuir*, 2009, **25**, 11078-11081.
49. Q. Peng, Y. Li, X. He, X. Gui, Y. Shang, C. Wang, C. Wang, W. Zhao, S. Du, E. Shi, P. Li, D. Wu and A. Cao, *Adv. Mater.*, 2014, **26**, 3241-3247.